Hindered Axial−Equatorial Carbonyl Exchange in an $Fe(CO)_4(PR_3)$ Complex of a Rigid Bicyclic Phosphine

Thomas S. Barnard and Mark R. Mason*

Department of Chemistry, University of Toledo, Toledo, Ohio 43606-3390

Received December 6, 2000

Variable-temperature ^{13}C NMR spectra for a series of $Fe(CO)_4(PR_3)$ complexes ligated by phosphatri(3-methylindolyl)methane (**1**), phosphatri(pyrrolyl)methane (**2**), P(*N*-3-methylindolyl)$_3$ (**3**), and P(*N*-pyrrolyl)$_3$ (**4**) are reported. Ligand **2** was prepared by reaction of tri(pyrrolyl)methane with PCl_3 in THF and Et_3N. Compound **2** is stable to methanolysis, hydrolysis, and aerial oxidation at room temperature. Reactions of **2** with selenium powder and $Rh(acac)(CO)_2$ yield phosphatri(pyrrolyl)methane selenide (**5**) and Rh(acac)(CO)(**2**) (**6**), respectively. The carbonyl stretching frequency in the IR spectrum of **6** and the magnitude of $^1J_{Se-P}$ in the ^{31}P NMR spectrum of **5** indicate that **2** is a strong π-acid and a weak σ-base, commensurate with its lack of reactivity with CH_3I. The trend in the decreasing basicity of **2** and related phosphines and phosphites was determined to be $P(NMe_2)_3$ > **3** > **4** > **1** > $P(OPh)_3$ > **2**. IR data for a series of Rh(acac)(CO)(PR_3) complexes indicate the trend in decreasing π-acceptor ability to be **2** ≈ **1** > **4** > $P(OPh)_3$ > **3** > PPh_3. Phosphines **1**−**4** were reacted with $Fe_2(CO)_9$ to yield $Fe(CO)_4$(**1**) (**7**), $Fe(CO)_4$(**2**) (**8**), $Fe(CO)_4$(**3**) (**9**), and $Fe(CO)_4$(**4**) (**10**), respectively. IR data for **7**−**10** support the trend in π-acidity listed above. Variable-temperature ^{13}C NMR spectra for compounds **8**−**10** show a single doublet resonance for the carbonyls in the temperature range from −80 to 20 °C indicative of rapid intramolecular rearrangement of carbonyls between axial and equatorial sites. However, the ^{13}C NMR spectrum for **7** shows slowed axial−equatorial carbonyl exchange at 20 °C. The limiting slow-exchange spectrum is observed at −20 °C. Hindered carbonyl exchange in **7** is attributed to the rigid 3-fold symmetry and steric bulk of **1**. In addition to characterization of the new compounds by NMR (^1H, ^{13}C, and ^{31}P) spectroscopy, IR spectroscopy, mass spectrometry, and elemental analysis, compounds **2**, **7**, **9**, and **10** were further characterized by X-ray crystallography.

Introduction

Intramolecular rearrangement in five-coordinate $Fe(CO)_4(PR_3)$ complexes is well-studied, and in nearly all cases exchange of axial and equatorial carbonyls is rapid relative to the ^{13}C NMR time scale.[1−9] For example, Whitmire and Lee were unable to observe limiting slow-exchange spectra down to −90 °C for a series of $Fe(CO)_4(PR_3)$ complexes (PR_3 = PMe_3, PPh_3, PCy_3, $P(OMe)_3$, and $P(OPh)_3$),[5] and Gansow and co-workers have shown that $Fe(CO)_4(PPh_3)$ remains fluxional at −110 °C.[6] This is analogous to the rapid exchange of carbonyls observed in $Fe(CO)_4$(py) and $Fe(CO)_5$ at temperatures of −100 and −170 °C, respectively.[7,8]

In contrast, Howell and co-workers did obtain a limiting slow-exchange ^{13}C NMR spectrum for $Fe(CO)_4${P(*o*-tolyl)$_3$} at −75 °C.[9] The carbonyl resonances coalesce at −40 °C, and at room temperature the carbonyl ^{13}C resonance appears as a doublet as is normally observed for fast-exchange spectra of $Fe(CO)_4(PR_3)$ complexes. Howell attributed hindered axial−equatorial carbonyl exchange in $Fe(CO)_4${P(*o*-tolyl)$_3$} to steric rather than electronic influences. This claim is supported by ^1H and ^{13}C NMR data, which suggest that carbonyl exchange is dependent on the conformation of the P(*o*-tolyl)$_3$ ligand and, possibly, that carbonyl exchange is concerted with P−C bond rotation. No additional examples of hindered carbonyl exchange in $Fe(CO)_4(PR_3)$ complexes have been reported, although limiting slow-exchange spectra have been observed for related $[Bi\{Fe(CO)_4\}_4]^{3-}$ and $Fe(CO)_4$(alkene) complexes.[10,11]

We have recently synthesized phosphatri(3-methylindolyl)methane (**1**) as a strong π-accepting phosphine with unique steric demands and rigid, 3-fold symmetry.[12] Initial results of coordination chemistry with **1** indicate it to be an excellent ligand for stabilizing tetrahedral and trigonal bipyramidal geometries around a metal center. We have now utilized **1** for the synthesis of $Fe(CO)_4$(**1**) in which axial−equatorial carbonyl exchange is slow even at room temperature! In an effort to elucidate if this hindered exchange is the result of the steric or strong π-accepting properties of **1**, we report here the synthesis of the less bulky, strong π-acid phosphatripyrrolylmethane (**2**) and the synthesis and variable-temperature ^{13}C NMR spectra for a series of $Fe(CO)_4(PR_3)$ complexes ligated by **1**, **2**, P(*N*-3-methylindolyl)$_3$ (**3**), and P(*N*-pyrrolyl)$_3$ (**4**).[13−15]

* To whom correspondence should be addressed. E-mail: mmason5@uoft02.utoledo.edu.

(1) Udovich, C. A.; Clark, R. J.; Haas, H. *Inorg. Chem.* **1969**, *8*, 1066.
(2) Mann, B. E. *Chem. Commun.* **1971**, 1173.
(3) Shapley, J. R.; Osborn, J. A. *Acc. Chem. Res.* **1973**, *6*, 305.
(4) Rossi, A. R.; Hoffmann, R. *Inorg. Chem.* **1975**, *14*, 365.
(5) Whitmire, K. H.; Lee, T. R. *J. Organomet. Chem.* **1985**, *282*, 95.
(6) Gansow, O. A.; Burke, A. R.; Vernon, W. D. *J. Am. Chem. Soc.* **1972**, *94*, 2550.
(7) Cotton, F. A.; Troup, J. M. *J. Am. Chem. Soc.* **1974**, *96*, 3438.
(8) Jesson, J. P.; Meakin, P. *J. Am. Chem. Soc.* **1973**, *95*, 1344.
(9) (a) Howell, J. A. S.; Palin, M. G.; McArdle, P.; Cunningham, D.; Goldschmidt, Z.; Gottlieb, H. E.; Hezroni-Langerman, D. *Inorg. Chem.* **1991**, *30*, 4683. (b) Howell, J. A. S.; Palin, M. G.; McArdle, P.; Cunningham, D.; Goldschmidt, Z.; Gottlieb, H. E.; Hezroni-Langerman, D. *Inorg. Chem.* **1993**, *32*, 3493.
(10) Whitmire, K. H.; Lagrone, C. B.; Churchill, M. R.; Fettinger, J. C.; Biondi, L. V. *Inorg. Chem.* **1984**, *23*, 4227.
(11) Wilson, S. T.; Coville, N. J.; Shapley, J. R.; Osborn, J. A. *J. Am. Chem. Soc.* **1974**, *96*, 4038.
(12) Barnard, T. S.; Mason, M. R. *Organometallics* **2001**, *20*, 206.
(13) Moloy, K. G.; Petersen, J. L. *J. Am. Chem. Soc.* **1995**, *117*, 7696.

10.1021/ic001372b CCC: $20.00
Published on Web 08/16/2001

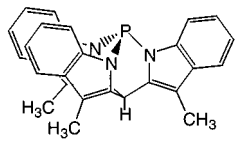

1

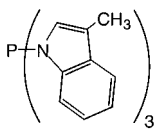

3

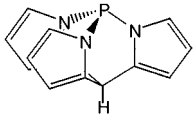

2

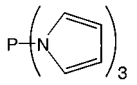

4

Experimental Section

General Procedures. All reactions were performed under an inert atmosphere of purified nitrogen using standard inert-atmosphere techniques unless otherwise specified. THF and hexanes were distilled from sodium benzophenone ketyl, and pyrrole was distilled from calcium hydride prior to use. Methanol and dichloromethane were degassed by nitrogen purge. $CDCl_3$ was dried by storage over activated molecular sieves. $RhCl_3 \cdot xH_2O$, $Fe_2(CO)_9$, and selenium powder were purchased from Strem Chemicals, Inc., and used as received. Phosphorus trichloride and triethyl orthoformate were purchased from Aldrich. Tri(pyrrolyl)methane,[16] $Rh(acac)(CO)_2$,[17] $Fe(CO)_4\{P(N\text{-pyrrolyl})_3\}$,[18] **1**,[12] and **3**[12] were prepared as described previously. Solution NMR spectra were recorded on a Varian VXRS400 spectrometer using $CDCl_3$ as the internal lock. Chemical shifts are reported relative to TMS (^1H, ^{13}C) or 85% H_3PO_4 (^{31}P). IR spectra were recorded on a Nicolet Fourier transform infrared (FT-IR) 5DX IR spectrometer. High-resolution mass spectrometric analyses were performed by the Mass Spectrometry Laboratory at The Ohio State University, Columbus, OH. Low-resolution mass spectral *m*/*z* values are reported for the predominant peak in the isotope pattern. Elemental analyses were performed by the Instrumentation Center in Arts and Sciences, The University of Toledo, Toledo, OH, or Schwarzkopf Microanalytical Laboratory, Inc., Woodside, NY.

Preparation of Phosphatri(pyrrolyl)methane (2). Tri(pyrrolyl)-methane (0.50 g, 2.37 mmol) was placed in a 100 mL three-neck flask. The flask was then charged with 25 mL of THF and 5 mL of NEt_3 (8.0 g, 79.0 mmol). A solution of 0.52 mL of PCl_3 (0.82 g, 6.0 mmol) in 5 mL of THF was added dropwise to the reaction solution at room temperature. A cloudy precipitate formed immediately, and the reaction mixture became dark green. The mixture was then heated to gentle reflux for 22 h. The dark green suspension was filtered to remove the precipitated solids, which were washed with THF (4 × 30 mL) until the washings were colorless. The combined clear green filtrates were taken to dryness in vacuo yielding a dark green solid residue. The solid was dissolved in diethyl ether (20 mL) and filtered in air to remove insoluble material, collecting the pale yellow filtrate. The yellow solution was concentrated to approximately 10 mL, and hexanes (10 mL) was added. The solution was cooled to −78 °C. The light tan fibrous solid was isolated by decantation of the supernatant liquid and dried under a stream of nitrogen. Yield: 0.187 g, 0.78 mmol, 33%. ^1H NMR ($CDCl_3$, 400 MHz): δ 6.97 (m, 3H, H5), 6.11 (d, 3H, H3, $^3J_{HH}$ = 3 Hz), 5.93 (q, 3H, H4, $^3J_{HH}$ = 3 Hz), 5.48 (s, 1H, CH). $^{13}C\{^1H\}$ NMR ($CDCl_3$, 100.6 MHz): δ 135.75 (s, C2), 120.67 (d, C5, $^2J_{PC}$ = 25.7 Hz), 109.49 (d, C4, $^3J_{PC}$ = 7.0 Hz), 105.53 (s, C3), 36.76 (s, CH). $^{31}P\{^1H\}$ NMR ($CDCl_3$, 161.9 MHz): δ 36.7 (s). MS (EI) *m*/*z* (assignment, relative intensity): 239 (M^+, 100), 193 ($M^+ - P - N -$ H, 7), 174 ($M^+ - C_4H_3N$, 2), 161 ($M^+ - C_4H_3N - CH$, 2). HRMS (EI) *m*/*z* for $C_{13}H_{10}N_3P$ (M^+): calcd 239.0612; found 239.0622. Anal. Calcd for $C_{13}H_{10}N_3P$: C, 65.27; H, 4.21; N, 17.57. Found: C, 64.06; H, 4.49; N, 17.37.

Preparation of Phosphatri(pyrrolyl)methane Selenide (5). A solution of **2** (0.200 g, 0.84 mmol) and selenium powder (0.290 g, 3.67 mmol) in 15 mL of toluene was refluxed for 18 h. The reaction solution was filtered through Celite, and the solvent and volatiles were removed in vacuo from the pale purple filtrate. The resulting residue was recrystallized in air from diethyl ether/hexanes (2:3 v/v) solution at −78 °C. The pale purple product was isolated by filtration, washed with cold hexanes (2 × 5 mL), and dried in air. Yield: 0.205 g, 0.64 mmol, 77%. ^1H NMR ($CDCl_3$, 400 MHz): δ 7.06 (m, 3H, H5), 6.19 (m, 3H, H3), 5.96 (m, 3H, H4), 5.53 (s, 1H, CH). $^{13}C\{^1H\}$ NMR ($CDCl_3$, 100.6 MHz): δ 136.47 (s, C2), 120.72 (d, C5, $^2J_{PC}$ = 9.2 Hz), 109.72 (d, C4, $^3J_{PC}$ = 12.9 Hz), 107.04 (d, C3, $^3J_{PC}$ = 6.2 Hz), 36.32 (d, CH, $^3J_{PC}$ = 4.1 Hz). $^{31}P\{^1H\}$ NMR ($CDCl_3$, 161.9 MHz): δ 28.3 ($^1J_{PSe}$ = 1032 Hz). MS (EI) *m*/*z* (assignment, relative intensity): 319 (M^+, 64), 239 ($M^+ - Se$, 100), 208 ($M^+ - Se - P$, 34), 174 ($M^+ - Se - P - C_4H_3N$, 30). HRMS (EI) *m*/*z* for $C_{13}H_{10}N_3P^{80}Se$ (M^+): calcd 318.9778; found 318.9794. Anal. Calcd for $C_{13}H_{10}N_3PSe$: C, 49.07; H, 3.17; N, 13.21. Found: C, 48.48; H, 3.02; N, 12.80.

Preparation of Rh(acac)(CO)(2) (6). To a solution of $Rh(acac)(CO)_2$ (0.043 g, 0.167 mmol) in 5 mL of CH_2Cl_2 was added **2** (0.040 g, 0.167 mmol) with immediate gas evolution. The yellow solution was stirred at room temperature for 1 h. The solvent was concentrated in vacuo to approximately 1 mL, and 8 mL of hexanes was added. The precipitated beige solid was isolated by decantation of the supernatant solution and dried under a stream of nitrogen. Yield: 0.068 g, 0.144 mmol, 87%. IR (ν_{CO}, cm^{-1}): 2024 (CH_2Cl_2); 2018, 2005 (KBr). ^1H NMR ($CDCl_3$, 400 MHz): δ 7.42 (s (br), 3H, H5), 6.13 (d, 3H, H3, $^3J_{HH}$ = 3 Hz), 5.94 (m, 3H, H4), 5.72 (s, 1H, CH), 5.50 (s, 1H, CH), 2.23 (s, 3H, CH_3), 2.09 (s, 3H, CH_3). $^{13}C\{^1H\}$ NMR ($CDCl_3$, 100.6 MHz): δ 188.11 (s, C═O), 185.88 (s, C═O), 185.24 (dd, Rh−CO, $^1J_{RhC}$ = 69.7 Hz, $^2J_{PC}$ = 34.5 Hz), 136.37 (d, C2), 125.65 (d, C5, $^2J_{PC}$ = 14.2 Hz), 109.32 (d, C4, $^3J_{PC}$ = 10.0 Hz), 105.73 (d, C3, $^3J_{PC}$ = 4.2 Hz), 101.08 (d, CH, $^4J_{PC}$ = 2.1 Hz), 36.54 (d, CH, $^3J_{PC}$ = 2.4 Hz), 27.39 (d, CH_3, $^4J_{PC}$ = 7.9 Hz), 26.55 (s, CH_3). $^{31}P\{^1H\}$ NMR ($CDCl_3$, 161.9 MHz): δ 78.6 (d, $^1J_{RhP}$ = 243.6 Hz). Anal. Calcd for $C_{34}H_{29}N_3O_3PRh$: C, 48.63; H, 3.65; N, 8.96. Found: C, 48.37; H, 3.71; N, 8.91.

Preparation of $Fe(CO)_4$(1) (7). A solution of **1** (1.0 g, 2.32 mmol) in 20 mL of toluene was added to a stirred suspension of $Fe_2(CO)_9$ (2.4 g, 6.60 mmol) in 20 mL of toluene at room temperature. The reaction solution quickly became green and was stirred at room temperature for 7 days. The resulting solution was filtered through Celite, and the solvent and volatiles were removed from the filtrate in vacuo. The green solid residue was chromatographed on a silica gel column (22 cm × 2.5 cm) using a 9:1 hexanes/CH_2Cl_2 solvent mixture to elute a green band, identified as $Fe_3(CO)_{12}$ (12 mg), followed by elution with a 1:4 hexanes/CH_2Cl_2 solvent mixture, which eluted a yellow band. Removal of the solvent in vacuo left a yellow solid, which was recrystallized from a hexanes/dichloromethane (2:1 v/v) solution at 0 °C as the solvate $Fe(CO)_4$(**1**)·$0.5CH_2Cl_2$. The yellow crystalline solid was isolated by filtration and washed with cold hexanes (3 × 10 mL). Yield: 1.15 g, 1.79 mmol, 77%. IR (hexane, ν_{CO}, cm^{-1}): 2076 (m), 2006 (m), 1977 (vs). ^1H NMR ($CDCl_3$, 400 MHz): δ 8.37 (d, 3H, H7, $^3J_{HH}$ = 8 Hz), 7.42 (d, 3H, H4, $^3J_{HH}$ = 8 Hz), 7.27 (t, 3H, H6, $^3J_{HH}$ = 8 Hz), 7.18 (t, 3H, H5, $^3J_{HH}$ = 8 Hz), 5.95 (s, 1H, CH), 5.28 (s, 1H, CH_2Cl_2), 2.40 (s, 9H, CH_3). $^{13}C\{^1H\}$ NMR (CD_2Cl_2, 100.6 MHz, −40 °C): δ 217.28 (d, Fe−CO_{ax}, $^2J_{PC}$ = 27.4 Hz), 207.12 (d, Fe−CO_{eq}, $^2J_{PC}$ = 40.2 Hz), 136.93 (d, C7a, $^2J_{PC}$ = 9.6 Hz), 134.48 (s, C2), 130.65 (d, C3a, $^3J_{PC}$ = 7.9 Hz), 123.38 (s, aryl), 121.77 (s, aryl), 119.58 (s, aryl), 112.52 (s, C7), 109.79 (s, C3), 30.63 (s, CH), 8.33 (s, CH_3). $^{31}P\{^1H\}$ NMR ($CDCl_3$, 161.9 MHz): δ 121.0 (s). Anal. Calcd for $C_{32}H_{22}N_3O_4PFe \cdot 0.5CH_2Cl_2$: C, 60.82; H, 3.61; N, 6.55. Found: C, 61.06; H, 3.41; N, 6.56.

Preparation of $Fe(CO)_4$(2) (8). A solution of **2** (0.20 g, 0.84 mmol) in 25 mL of diethyl ether was added to $Fe_2(CO)_9$ (0.30 g, 0.83 mmol) in a 100 mL Schlenk flask at room temperature. The orange suspension was stirred at room temperature for 18 h becoming tan in color. The

(14) Fischer, S.; Hoyano, J.; Johnson, I.; Peterson, L. K. *Can. J. Chem.* **1976**, *54*, 2706.
(15) Issleib, K.; Brack, A. *Z. Anorg. Allg. Chem.* **1957**, *292*, 245.
(16) (a) Wang, Q. M.; Bruce, D. W. *Synlett* **1995**, 1267. (b) Mason, M. R.; Barnard, T. S.; Bensaid, L.; Segla, M. F.; Xie, B. Manuscript in preparation.
(17) Varshavskii, Yu. S.; Cherkasova, T. G. *Russ. J. Inorg. Chem. (Engl. Transl.)* **1967**, *12*, 1709.
(18) Atwood, J. L.; Cowley, A. H.; Hunter, W. E.; Mehrotra, S. K. *Inorg. Chem.* **1982**, *21*, 1354.

solvent and volatiles were removed in vacuo. The tan solid residue was dissolved in CH_2Cl_2 and filtered. The solution was concentrated in vacuo, and twice the volume of hexanes was added. The solution was cooled to −25 °C. The light yellow solid was isolated by filtration, washed with cold hexanes (2 × 5 mL), and dried in air. Yield: 0.205 g, 0.50 mmol, 60%. IR (hexane, ν_{CO}, cm^{-1}): 2078 (m), 2012 (m), 1980 (vs). ^1H NMR ($CDCl_3$, 400 MHz): δ 6.99 (m, 3H, H5), 6.20 (m, 3H, H3), 6.00 (m, 3H, H4), 5.56 (s, 1H, CH). $^{13}C\{^1H\}$ NMR (CD_2Cl_2, 100.6 MHz, −80 °C): δ 208.59 (d, Fe−CO, $^2J_{PC}$ = 23.6 Hz), 135.08 (s, C2), 120.72 (d, C5, $^2J_{PC}$ = 13.7 Hz), 109.55 (d, C4, $^3J_{PC}$ = 10.4 Hz), 106.57 (s, C3), 35.32 (s, CH). $^{31}P\{^1H\}$ NMR ($CDCl_3$, 161.9 MHz): δ 134.4 (s). Anal. Calcd for $C_{17}H_{10}N_3O_4PFe$: C, 50.15; H, 2.48; N, 10.32. Found: C, 50.39; H, 2.52; N, 10.40.

Preparation of $Fe(CO)_4$(3) (9). A solution of **3** (0.625 g, 1.48 mmol) in 25 mL of toluene was added to $Fe_2(CO)_9$ (0.54 g, 1.48 mmol) in a 100 mL Schlenk flask at room temperature. The orange suspension was stirred at room temperature for 18 h becoming light brown in color. The solvent and volatiles were removed in vacuo. The orange-yellow solid residue was dissolved in CH_2Cl_2 and filtered. The solution was concentrated in vacuo, and three times the volume of hexanes was added. The solution was cooled to −25 °C. The orange-yellow solid was isolated by filtration, washed with cold hexanes (2 × 5 mL), and dried in air. Yield: 0.784 g, 1.33 mmol, 90%. IR (hexane, ν_{CO}, cm^{-1}): 2065 (m), 1997 (m), 1966 (vs). ^1H NMR ($CDCl_3$, 400 MHz): δ 7.57 (d, 3H, H7, $^3J_{HH}$ = 8 Hz), 7.27 (d, 3H, H4, $^3J_{HH}$ = 8 Hz), 7.25 (t, 3H, H6, $^3J_{HH}$ = 8 Hz), 7.15 (t, 3H, H5, $^3J_{HH}$ = 8 Hz), 6.52 (d, 3H, H2, $^2J_{PC}$ = 3.2 Hz), 2.23 (s, 9H, CH_3). $^{13}C\{^1H\}$ NMR (CD_2Cl_2, 100.6 MHz, −50 °C): δ 211.38 (d, Fe−CO, $^2J_{PC}$ = 19.9 Hz), 137.13 (d, C7a, $^2J_{PC}$ = 4.5 Hz), 132.86 (d, C3a, $^3J_{PC}$ = 5.4 Hz), 124.74 (d, C2, $^2J_{PC}$ = 4.9 Hz), 123.72 (s, aryl), 122.38 (s, aryl), 119.77 (s, aryl), 118.08 (d, C3, $^3J_{PC}$ = 5.8 Hz), 114.10 (s, C7), 9.62 (s, CH_3). $^{31}P\{^1H\}$ NMR ($CDCl_3$, 161.9 MHz): δ 143.9 (s). Anal. Calcd for $C_{31}H_{24}N_3O_4PFe$: C, 63.18; H, 4.10; N, 7.13. Found: C, 63.69; H, 4.13; N, 7.11.

Reaction of 2 with Methyl Iodide. Compound **2** (0.054 g, 0.226 mmol) was dissolved in 5 mL of toluene in a Schlenk flask. To the solution was added methyl iodide (0.10 mL, 1.6 mmol) via syringe. The reaction solution was stirred at room temperature for 2 days. There was no precipitate formed during this time. The solvent and volatiles were removed in vacuo, and the remaining white solid residue was identified as unreacted **2** by ^1H and ^{31}P NMR spectroscopy.

Reaction of 2 with Methanol. Approximately 10 mg of **2** was dissolved in $CDCl_3$ in an NMR tube, followed by addition of 2 drops of wet methanol. The NMR tube was allowed to stand at room temperature and was monitored by ^1H and ^{31}P NMR spectroscopy over a period of 5 days. During this time, **2** was unchanged.

Crystallographic Analyses. Crystals of **2** suitable for X-ray diffraction analysis were grown from a 1:1 hexane/dichloromethane solvent mixture by slow evaporation at room temperature. Crystals of **9** and $Fe(CO)_4$(**4**) (**10**) were grown from 3:1 hexane/dichloromethane and 1:1 chloroform/heptane solvent mixtures, respectively, at room temperature. Crystals of **7** were grown from a 2:1 hexane/dichloromethane solution at 0 °C. Preliminary examination and data collection were carried out, at room temperature for **2**, **9**, and **10** and at 150 K for **7**, on a Siemens SMART Platform diffractometer with a CCD detector. Preliminary orientation matrix and unit cell parameters were determined by collecting 60 20-s frames, followed by spot integration and least-squares refinement. Intensity data were collected using 0.3° ω-scans at three different ϕ-settings corresponding to a nominal sphere of data. Frames were integrated using the SAINT program. The intensities of the reflections were corrected for absorption and decay (SADABS).[19] Equivalent reflections were averaged, and all unique data were used for additional calculations. The structures were solved by direct methods (SHELXS-86).[20] All non-hydrogen atoms were refined with anisotropic thermal parameters by full matrix least-squares on F^2 using all unique data (SHELXL-93).[21] The hydrogen atoms in **2**, **7**, and **10** were located and refined with isotropic thermal parameters. The solution of **9** showed orientational disorder of one 3-methylindolyl substituent over two positions with occupancies of 82% and 18%. The hydrogen atoms in **9** were located and refined isotropically with the exception of the hydrogen atoms of the disordered indolyl group, which were included with idealized geometry. Crystals of **7** contained 0.5 equiv of CH_2Cl_2 from the crystallization solvent. The disordered molecule was included in the analysis and satisfactorily refined. Crystallographic data are summarized in Table 1.

Table 1. Crystal Data and Structure Refinement Details for **2**, **7**, **9**, and **10**

	2	**7**	**9**	**10**
formula	$C_{13}H_{10}N_3P$	$C_{32}H_{22}FeN_3O_4P\cdot 0.5CH_2Cl_2$	$C_{31}H_{24}FeN_3O_4P$	$C_{16}H_{12}FeN_3O_4P$
fw	239.21	641.81	589.35	397.11
space group	$P2_12_12_1$	$P\bar{1}$	$Pcab$	$P\bar{1}$
a, Å	7.9347(5)	10.4807(16)	8.7425(7)	9.1920(3)
b, Å	7.9781(5)	11.3083(14)	18.0742(13)	10.2470(8)
c, Å	17.9210(11)	14.506(2)	35.872(3)	10.7407(3)
α, deg		82.139(5)		86.360(5)
β, deg		72.167(5)		65.577(4)
γ, deg		62.857(4)		88.141(4)
V, Å^3	1134.47(12)	1456.4(4)	5668.2(7)	919.27(8)
Z	4	2	8	2
D_{calcd}, g cm^{-3}	1.401	1.464	1.381	1.435
T, °C	20(2)	−123(1)	20(2)	20(2)
μ, mm^{-1}	0.220	0.708	0.630	0.931
λ, Å	0.71 073	0.71 073	0.71 073	0.71 073
R_1[a] (F, $I > 2\sigma(I)$)	0.0307	0.0386	0.0533	0.0426
wR2 [b] (F^2, all data)	0.0831	0.1020	0.1105	0.1104

[a] $R_1(F) = \sum ||F_o| - |F_c|| / \sum |F_o|$. [b] $wR2\ (F^2) = [\sum[w(F_o^2 - F_c^2)^2] / \sum[w(F_o^2)^2]]^{1/2}$.

Results and Discussion

Synthesis, Characterization, and Electronic Properties of 2. To assess steric effects on the carbonyl exchange in **7** required the synthesis of a constrained, bicyclic phosphine with similar electronic properties to those for ligand **1** but with reduced steric requirements. With this aim, the constrained phosphine **2** was synthesized by reaction of tri(pyrrolyl)methane[16] with 2.5 equiv of PCl_3 in the presence of triethylamine (eq 1). An excess of PCl_3 was required to ensure complete consumption of tri(pyrrolyl)methane during the reaction. Recrystallization from diethyl ether/hexanes gave **2** in 33% yield. Compound **2** has been characterized by mass spectrometry, NMR spectroscopy, and X-ray crystallography.

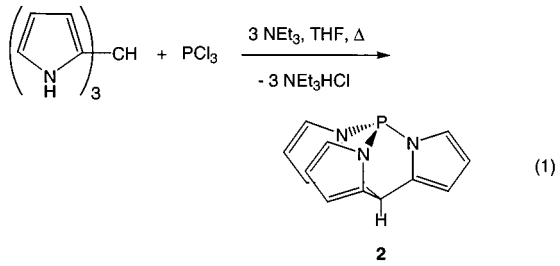

(1)

2

As previously found for **1**,[12] ^{13}C and ^{31}P NMR spectra provide valuable information in determining the atom connectivity of **2**. The magnitude of the $^{31}P-^{13}C$ coupling constants is known to depend on the proximity of the coupled carbon atom to the phosphorus lone pair. Coupling is large when the carbon atom is close to the lone pair and small when the carbon atom is remote. This lone pair orientation effect is most apparent in rigid bicyclic phosphines such as phosphatriptycene[22] and 1,6-diphosphatriptycene.[23] The ^{13}C NMR spectrum of the rigid

(19) Sheldrick, G. M. *SADABS: Absorption Correction Program*; University of Göttingen: Göttingen, Germany, 1996.
(20) Sheldrick, G. M. *Acta Crystallogr.* **1990**, *A46*, 467.
(21) Sheldrick, G. M. *SHELXL-93: Program for Refinement of Crystal Structures*; University of Göttingen: Göttingen, Germany, 1993.
(22) Jongsma, C.; de Kleijn, J. P.; Bickelhaupt, F. *Tetrahedron* **1974**, *30*, 3465.
(23) Sørensen, S.; Jakobsen, H. J. *Org. Magn. Reson.* **1977**, *9*, 101.

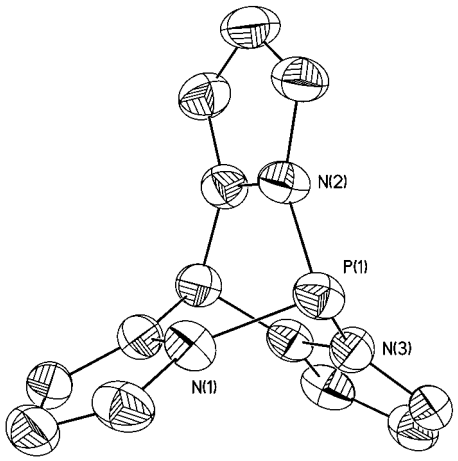

Figure 1. ORTEP drawing of phosphatri(pyrrolyl)methane (**2**). Thermal ellipsoids are drawn at the 50% probability level. Hydrogen atoms are omitted for clarity.

Table 2. Selected Bond Distances (Å) and Angles (deg) for **2**

Distances		Angles	
P(1)−N(1)	1.7388(14)	N(1)−P(1)−N(2)	94.03(6)
P(1)−N(2)	1.7270(14)	N(1)−P(1)−N(3)	94.14(6)
P(1)−N(3)	1.7266(13)	N(2)−P(1)−N(3)	94.23(7)

bicyclic phosphine **2** similarly exhibits lone pair orientation effects which are reflected in the $^{31}P-^{13}C$ coupling constants. Specifically, $^{2}J_{P-C5}$ is large (25.7 Hz), while $^{2}J_{P-C2}$ is negligible (∼0 Hz), and $^{3}J_{P-C4}$ (7.0 Hz) is larger than $^{3}J_{P-C3}$ (∼0 Hz). This pattern of $^{31}P-^{13}C$ coupling constants is consistent with the bridgehead methine group imposing constraint of the pyrrolyl substituents.

In addition, the ^{31}P NMR spectrum also provides informative data concerning the structure of **2**. The ^{31}P chemical shift of **2** (36.7 ppm) is 42.9 ppm upfield of that for **4** (79.6 ppm)[13] due to the increased s character of the phosphorus lone pair that results from a decrease of the N−P−N angles upon constraint of the pyrrolyl substituents by the bridgehead methine group of **2**. A similar upfield shift of the ^{31}P NMR resonance upon substituent constraint has been noted for phosphine **1** (22.3 ppm) compared with **3** (64.7 ppm),[12] as well as for the series 1,6-diphosphatriptycene (−43 ppm),[24] phosphatriptycene (−64 ppm),[22] and azaphosphatriptycene (−80 ppm),[25] where the bridgehead atom decreases in size, reducing the C−P−C angles.

The molecular structure of **2** was further confirmed by X-ray crystallography. An ORTEP diagram of **2** is shown in Figure 1 and selected bond distances and angles are given in Table 2. The structure consists of a central bicyclic framework with the phosphorus atom bonded to the nitrogen atoms of the pyrrolyl groups. The sum of the N−P−N angles is 282.4°, considerably less than the sum for **4** (301.2°)[18] and P(*N*-indolyl)$_3$ (299.8°)[26] but comparable to the sum of the N−P−N angles for **1** (285.3°).[12] The P−N bond distances in **2** average to a value of 1.731 Å, which is slightly longer than the average of P−N bond distances for **4** (1.696 Å),[18] P(*N*-indolyl)$_3$ (1.709 Å),[26] and **1** (1.708 Å).[12] The three nitrogen atoms are planar, as expected for sp^2 hybridization, with an averaged sum of angles about the nitrogen atoms of 359.7°. The pyrrolyl groups are planar within experimental error. The molecule has pseudo-3-fold symmetry along the methine C−P axis, although in the solid state the angles between the pyrrolyl groups show some deviation from C_{3v} symmetry with an angle of 128.3(1)° between the N(2) and N(3) pyrrolyl groups. This increased angle results in the reduction of the angle between the N(1) and N(3) pyrrolyl groups to 113.2(1)°, while the remaining angle between the N(2) and N(3) groups is 118.5(1)°.

Table 3. $^{31}P-^{77}Se$ Coupling Constants for Selenophosphates and Phosphine Selenides

	$^{1}J_{31P-77Se}$ (Hz)	ref
Se=P(OCH$_2$)$_2$COMe	1099	28
Se=P(OCH$_2$)$_3$CCH$_3$	1053	28
Se=**2** (**5**)	1032	*a*
Se=P(OPh)$_3$	1025	29
Se=P(OCH$_2$CH$_2$O)(OMe)	1011	28
Se=**1**	1008	12
Se=**4**	970	12
Se=P(OMe)$_3$	954	28
Se=**3**	943	12
Se=P(NMeCH$_2$)$_3$CCH$_3$	854	28
Se=P(NMe$_2$)$_3$	784	28
Se=PPh$_3$	735	30

[a] This work.

As was found for **1**,[12] **3**,[12] and **4**,[13−15] compound **2** is stable to aerial oxidation and the P−N bonds are stable to moisture and methanol. In addition, reaction with CH_3I did not result in the formation of the corresponding phosphonium salt, indicative of the reduced basicity of **2**. The lack of reactivity with CH_3I suggests that **2** is a poor σ-donor and possibly a good π-acceptor, as are phosphines **1**, **3**, and **4**. Hence, the electronic properties and the effects of constraint by the tri(pyrrolyl)methane framework were assessed by qualitative comparison of the $^{1}J_{P-Se}$ value for the selenide derivative and ν_{CO} data for the Rh(acac)(CO)(PR$_3$) complex of **2** with those of **1**, **3**, and **4**.

Verkade and co-workers have shown that increasing the geometric constraint of substituents and the concomitant reduction of O−P−O angles for a series of phosphites results in decreased σ-basicity, as indicated by an increase in the $^{31}P-^{77}Se$ coupling constants of the corresponding selenophosphates.[27−29] Reduced σ-basicity was also noted for P(CH$_3$NCH$_2$)$_3$CCH$_3$ in comparison to the noncyclic tris(dimethylamino)phosphine, based again on the $^{31}P-^{77}Se$ coupling constants of the respective selenide derivatives.[28] We previously utilized the $^{31}P-^{77}Se$ coupling constants to qualitatively compare the basicity of **1** with that of **3** and other selenophosphates and phosphine selenides (Table 3).[12,28−30] The increased $^{31}P-^{77}Se$ coupling constant for **1**=Se relative to other phosphine selenides results from increased s character in the P−Se bond. Similarly, the increased s character of the phosphorus lone pair accounts for the poor σ-donor properties of **1**.

The reaction of **2** with Se powder in refluxing toluene was complete in 18 h and gave phosphine selenide **5** in 77% yield upon recrystallization (eq 2). High-resolution mass spectrometry

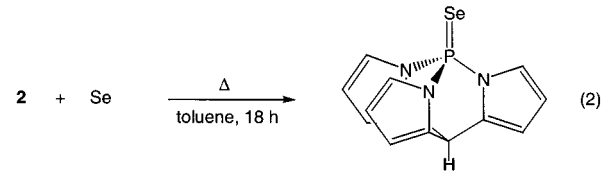

(2)

and elemental analysis confirmed the proposed composition of **5**, and atom connectivity was confirmed by NMR (^{1}H, ^{13}C, and

(24) Weinberg, K. G.; Whipple, E. B. *J. Am. Chem. Soc.* **1971**, *93*, 1801.
(25) Hellwinkel, D.; Schenk, W. *Angew. Chem., Int. Ed. Engl.* **1969**, *8*, 987.
(26) Frenzel, A.; Gluth, M.; Herbst-Irmer, R.; Klingebiel, U. *J. Organomet. Chem.* **1996**, *514*, 281.

Table 4. Carbonyl Stretching Frequencies for $Rh(acac)(CO)(PR_3)$ Complexes

PR_3	ν_{CO} (cm^{-1}) (CH_2Cl_2)	PR_3	ν_{CO} (cm^{-1}) (CH_2Cl_2)
2	2024	$PPh(NC_4H_4)_2$	2002[b]
1	2024[a]	$PPh_2(NC_4H_4)$	1990[b]
$P(NC_4H_4)_3$ (**4**)	2012[b]	$P(p\text{-}CF_3C_6H_4)_3$	1986[b]
$P(OPh)_3$	2008[b]	$P(p\text{-}FC_6H_4)_3$	1980[b]
3	2005[a]	PPh_3	1978[b]

[a] Reference 12. [b] Reference 32.

^{31}P) spectroscopy. The $^{31}P-^{77}Se$ coupling constant of **5** (1032 Hz) is larger than the value found for $Se{=}P(N\text{-pyrrolyl})_3$ (970 Hz),[12] which is consistent with decreased σ-basicity of the phosphorus lone pair upon constraint of the pyrrolyl substituents by the bicyclic tri(pyrrolyl)methane framework of **5**. The $^1J_{P-Se}$ value for **5** is slightly greater than that of $Se{=}P(OPh)_3$ ($^1J_{P-Se}$ = 1025 Hz),[29] indicating that the σ-basicity of **2** is slightly less than that of $P(OPh)_3$. Thus, the trend in decreasing basicity is $P(NMe_2)_3$ > **3** > **4** > **1** > $P(OPh)_3$ > **2**.

The π-acidity of **2** was assessed by comparison of ν_{CO} data for a series of $Rh(acac)(CO)(PR_3)$ complexes (Table 4). Ziolkowski and co-workers recently reported the synthesis of the monosubstituted Rh(acac)(CO)(**4**) by reaction of **4** with $Rh(acac)(CO)_2$.[31] Similarly, we have prepared Rh(acac)(CO)(**2**) (**6**) in 87% yield (eq 3). The carbonyl stretch of **6** is observed at

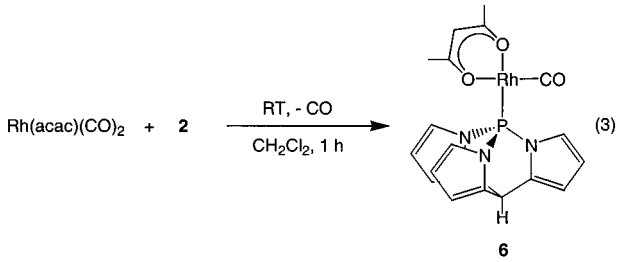

(3)

6

2024 cm^{-1}, higher than those for Rh(acac)(CO)(**4**) (2012 cm^{-1}) and Rh(acac)(CO){$P(OPh)_3$} (2008 cm^{-1}),[32] which indicates the stronger π-acceptor properties of **2**. But the ν_{CO} value for **6** is the same as that of Rh(acac)(CO)(**1**) (2024 cm^{-1}),[12] suggesting that the π-acidity of **1** and **2** is similar despite the slightly better electron-withdrawing ability of the pyrrolyl group. The difference in the electron-withdrawing abilities of the pyrrolyl and indolyl groups is apparent in the difference between the ν_{CO} values for Rh(acac)(CO)(**4**) (2012 cm^{-1})[32] and Rh(acac)(CO)(**3**) (2005 cm^{-1}).[12] On the basis of the ν_{CO} data, the phosphines can be arranged in the following order of decreasing π-acidity: **1** ≈ **2** > **4** > $P(OPh)_3$ > **3** > PPh_3.

Synthesis and Characterization of $Fe(CO)_4(PR_3)$ Complexes 7−10. Reactions of $Fe_2(CO)_9$ with compounds **1**−**3** yield yellow, crystalline complexes $Fe(CO)_4$(**1**) (**7**), $Fe(CO)_4$(**2**) (**8**), and $Fe(CO)_4$(**3**) (**9**), respectively (Scheme 1). $Fe(CO)_4$(**4**) (**10**) was similarly prepared by reaction of $Fe_2(CO)_9$ with **4** as described by Atwood and co-workers,[18] although in our hands yields were somewhat lower than those reported and a second phosphine carbonyl complex was separated from the crude reaction product. Nonetheless, spectroscopic data on recrystallized **10** are in agreement with those reported by Atwood. Compounds **7**−**10** each show a single ^{31}P NMR resonance and ^1H and ^{13}C NMR spectra consistent with the proposed axial-substituted complexes.

Scheme 1

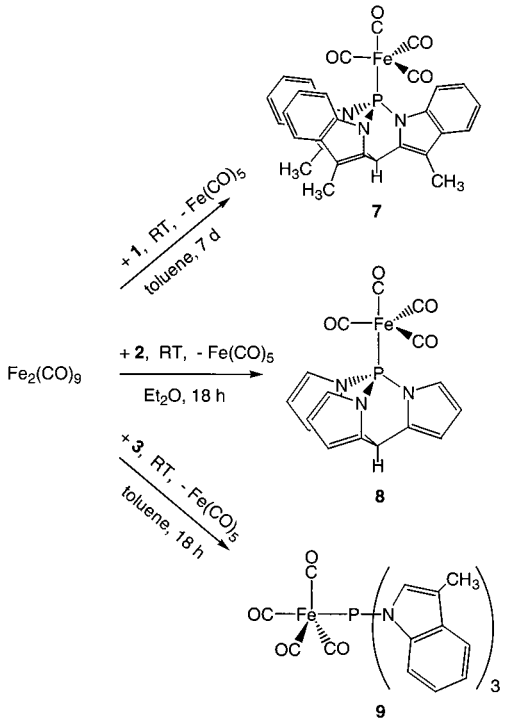

Table 5. Carbonyl Stretching Frequencies for $Fe(CO)_4(PR_3)$ Complexes

PR_3	ν_{CO} (cm^{-1})[a]	ref
2	2078, 2012, 1980	*d*
1	2076, 2006, 1977	*d*
$P(NC_4H_4)_3$ (**4**)	2070, 2005, 1970	*d*
ADPO	2070, 2005, 1977[b]	33
$P(OCH_2)_3CCH_3$	2070, 1997, 1970	34
$P(OPh)_3$	2068, 1997, 1963	35
3	2065, 1997, 1966	*d*
$P(OMe)_3$	2065, 1992, 1966	1
$P(3,5\text{-}(CF_3)_2C_6H_3)_3$	2063, 1995, 1955	36
$P(MeNCH_2)_3CCH_3$	2058, 1985, 1951[c]	37
PMe_3	2053, 1979, 1938	35
PPh_3	2052, 1979, 1947	34
$P(p\text{-}CF_3C_6H_4)_3$	2051, 1985, 1949	36
PEt_3	2051, 1976, 1938	35
$P(NMe_2)_3$	2048, 1973, 1936[c]	37

[a] Spectra obtained in hexane solution unless otherwise indicated. [b] Pentane. [c] Cyclohexane. [d] This work.

Previously unreported IR ν_{CO} data for **10** as well as ν_{CO} data for new complexes **7**−**9** are given in Table 5. The solution IR spectra for compounds **7**−**10** each display three carbonyl stretches in the expected pattern for axial-substituted $Fe(CO)_4(PR_3)$ complexes of C_{3v} symmetry. The highest frequency A_1(eq) bands for compounds **7**−**10** are observed at 2076, 2078, 2065, and 2070 cm^{-1}, respectively. The relative positions of the A_1(eq) bands in compounds **7**−**10** and related $Fe(CO)_4(PR_3)$ complexes[1,33−37] indicate the order of decreasing π-acidity as **2** ≈ **1** > **4** > $P(OPh)_3$ > **3** > PPh_3 > $P(NMe_2)_3$, consistent with the order determined by IR data for $Rh(acac)(CO)(PR_3)$ complexes. The A_1(eq) band at 2070 cm^{-1} for **10** is equivalent to those reported for $Fe(CO)_4\{P(OCH_2)_3CCH_3\}$ and $Fe(CO)_4$-

(27) Verkade, J. G.; Mosbo, J. A. In *Phosphorus-31 NMR Spectroscopy in Stereochemical Analysis*; Verkade, J. G., Quin, L. D., Eds.; VCH Publishers: Deerfield Beach, FL, 1987; pp 453−455.
(28) Kroshefsky, R. D.; Weiss, R.; Verkade, J. G. *Inorg. Chem.* **1979**, *18*, 469.
(29) Socol, S. M.; Verkade, J. G. *Inorg. Chem.* **1984**, *23*, 3487.
(30) McFarlane, W.; Rycroft, D. S. *J. Chem. Soc., Dalton Trans.* **1973**, 2162.
(31) Trzeciak, A. M.; Glowiak, T.; Grzybek, R.; Ziolkowski, J. J. *J. Chem. Soc., Dalton Trans.* **1997**, 1831.
(32) Serron, S.; Huang, J.; Nolan, S. P. *Organometallics* **1998**, *17*, 534.

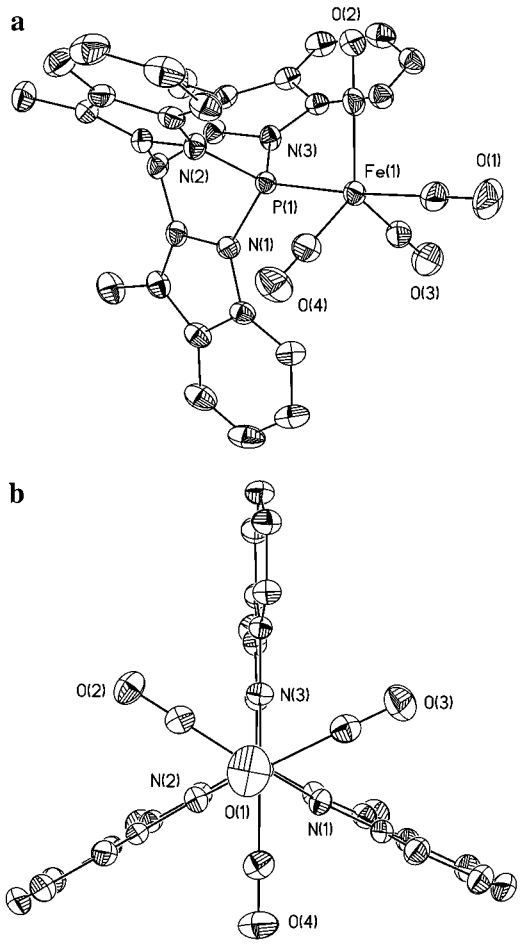

Figure 2. (a) ORTEP drawing of $Fe(CO)_4$(**1**) (**7**). Thermal ellipsoids are drawn at the 50% probability level. Hydrogen atoms are omitted for clarity. (b) ORTEP drawing of **7** viewed down the pseudo-3-fold C(1)−Fe(1)−P(1) axis.

(ADPO) (ADPO = 3,7-di-*tert*-butyl-5-aza-2,8-dioxa-1-phosphabicyclo[3.3.0]octa-2,4,6-triene) (Table 5), indicating that **4** has π-acceptor properties comparable to phosphites, whereas **1** and **2** are clearly stronger π-acceptors than phosphites. The data also suggest that compounds **1**−**4** are stronger π-acceptors than trifluoromethyl-substituted arylphosphines[36] and aminophosphines.[37]

Compounds **7**, **9**, and **10** were also characterized by X-ray crystallography. ORTEP diagrams of each molecule are shown in Figures 2−4. Selected bond distances and angles are listed in Tables 6−8. Each complex possesses approximate C_{3v} symmetry with the phosphine ligand occupying an axial position about the trigonal-bipyramidal iron, as expected, based on solution IR data and previously proposed π-back-bonding arguments.[4] The P(1)−Fe(1)−C(1) angles for **7**, **9**, and **10** are 176.06(6)°, 174.48(10)°, and 178.64(11)°, respectively, and the

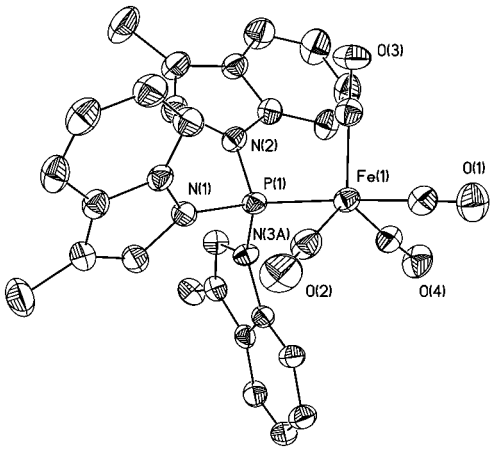

Figure 3. ORTEP drawing of $Fe(CO)_4$(**3**) (**9**). Thermal ellipsoids are drawn at the 30% probability level. Hydrogen atoms are omitted for clarity.

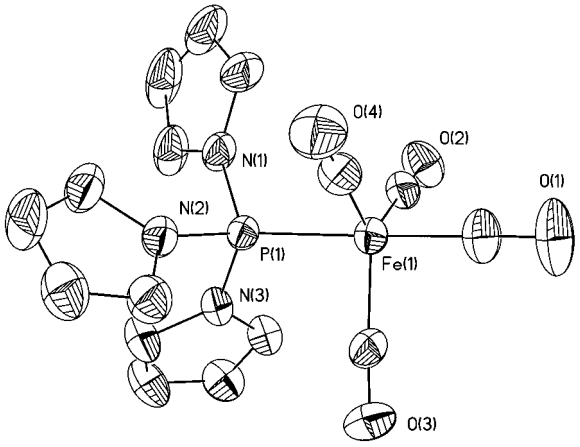

Figure 4. ORTEP drawing of $Fe(CO)_4$(**4**) (**10**). Thermal ellipsoids are drawn at the 30% probability level. Hydrogen atoms are omitted for clarity.

Table 6. Selected Bond Distances (Å) and Angles (deg) for **7**

Distances			
Fe(1)−P(1)	2.1539(5)	Fe(1)−C(1)	1.8151(19)
Fe(1)−C(2)	1.7943(18)	Fe(1)−C(3)	1.807(2)
Fe(1)−C(4)	1.7983(19)	P(1)−N(1)	1.7051(14)
P(1)−N(2)	1.7095(15)	P(1)−N(3)	1.7110(15)
O(1)−C(1)	1.133(2)	O(2)−C(2)	1.147(2)
O(3)−C(3)	1.143(3)	O(4)−C(4)	1.147(2)

Angles			
P(1)−Fe(1)−C(1)	176.06(6)	P(1)−Fe(1)−C(2)	86.09(6)
P(1)−Fe(1)−C(3)	93.31(6)	P(1)−Fe(1)−C(4)	89.26(6)
C(1)−Fe(1)−C(2)	90.02(8)	C(1)−Fe(1)−C(3)	89.22(9)
C(1)−Fe(1)−C(4)	92.30(9)	C(2)−Fe(1)−C(3)	121.18(8)
C(2)−Fe(1)−C(4)	122.00(9)	C(3)−Fe(1)−C(4)	116.79(9)
Fe(1)−P(1)−N(1)	121.55(5)	Fe(1)−P(1)−N(2)	117.95(5)
Fe(1)−P(1)−N(3)	119.67(5)	N(1)−P(1)−N(2)	97.17(7)
N(1)−P(1)−N(3)	98.03(7)	N(2)−P(1)−N(3)	97.36(7)
Fe(1)−C(1)−O(1)	178.5(2)	Fe(1)−C(2)−O(2)	179.32(15)
Fe(1)−C(3)−O(3)	176.61(19)	Fe(1)−C(4)−O(4)	179.63(18)

Fe−C and C−O distances are similar to those commonly observed in axial-substituted $Fe(CO)_4(PR_3)$ complexes.[9,33,36,38−43]

The most striking feature of each structure is the short Fe−P bond distances of **7** (2.1539(5) Å), **9** (2.1970(8) Å), and **10** (2.1661(7) Å). Iron−phosphorus distances in axial-substituted $Fe(CO)_4(PR_3)$ complexes range[9,33,36,38−43] from 2.158(3) Å in $Fe(CO)_4$(ADPO)[33] to 2.364(1) Å in $Fe(CO)_4(P^tBu_3)$.[39] The Fe−P distances in **7**, **9**, and **10** are considerably shorter than the corresponding distances in $Fe(CO)_4(PPh_3)$ (2.244(1) Å)[40] and

(33) Arduengo III, A. J.; Lattman, M.; Dixon, D. A. Calabrese, J. C. *Heteroat. Chem.* **1991**, *2*, 395.
(34) Martin, L. R.; Einstein, F. W. B.; Pomeroy, R. K. *Inorg. Chem.* **1985**, *24*, 1777.
(35) Van Rentergem, M.; Van Der Kelen, G. P.; Claeys, E. C. *J. Mol. Struct.* **1982**, *80*, 317.
(36) (a) Howell, J. A. S.; Fey, N.; Lovatt, J. D.; Yates, P. C.; McArdle, P.; Cunningham, D.; Sadeh, E.; Gottlieb, H. E.; Goldschmidt, Z.; Hursthouse, M. B.; Light, M. E. *J. Chem. Soc., Dalton Trans.* **1999**, 3015. (b) Howell, J. A. S.; Lovatt, J. D.; McArdle, P.; Cunningham, D.; Maimone, E.; Gottlieb, H. E.; Goldschmidt, Z. *Inorg. Chem. Commun.* **1998**, *1*, 118.
(37) Kroshefsky, R. D.; Verkade, J. G.; Pipal, J. R. *Phosphorus Sulfur Relat. Elem.* **1979**, *6*, 377.

Table 7. Selected Bond Distances (Å) and Angles (deg) for **9**

Distances			
Fe(1)−P(1)	2.1970(8)	Fe(1)−C(1)	1.791(3)
Fe(1)−C(2)	1.800(3)	Fe(1)−C(3)	1.799(3)
Fe(1)−C(4)	1.792(3)	P(1)−N(1)	1.696(2)
P(1)−N(2)	1.699(2)	P(1)−N(3A)	1.717(4)
O(1)−C(1)	1.136(3)	O(2)−C(2)	1.135(3)
O(3)−C(3)	1.132(3)	O(4)−C(4)	1.136(3)
Angles			
P(1)−Fe(1)−C(1)	174.48(10)	P(1)−Fe(1)−C(2)	88.20(11)
P(1)−Fe(1)−C(3)	91.25(10)	P(1)−Fe(1)−C(4)	93.62(10)
C(1)−Fe(1)−C(2)	86.30(14)	C(1)−Fe(1)−C(3)	91.32(13)
C(1)−Fe(1)−C(4)	89.80(13)	C(2)−Fe(1)−C(3)	123.07(13)
C(2)−Fe(1)−C(4)	122.88(13)	C(3)−Fe(1)−C(4)	113.97(13)
Fe(1)−P(1)−N(1)	115.91(9)	Fe(1)−P(1)−N(2)	117.81(9)
Fe(1)−P(1)−N(3A)	120.32(14)	N(1)−P(1)−N(2)	99.66(11)
N(1)−P(1)−N(3A)	102.18(17)	N(2)−P(1)−N(3A)	97.32(15)
Fe(1)−C(1)−O(1)	177.8(3)	Fe(1)−C(2)−O(2)	177.0(3)
Fe(1)−C(3)−O(3)	178.1(3)	Fe(1)−C(4)−O(4)	176.0(3)

Table 8. Selected Bond Distances (Å) and Angles (deg) for **10**

Distances			
Fe(1)−P(1)	2.1661(7)	Fe(1)−C(1)	1.793(3)
Fe(1)−C(2)	1.786(3)	Fe(1)−C(3)	1.778(3)
Fe(1)−C(4)	1.787(3)	P(1)−N(1)	1.688(2)
P(1)−N(2)	1.698(2)	P(1)−N(3)	1.691(2)
O(1)−C(1)	1.139(4)	O(2)−C(2)	1.139(3)
O(3)−C(3)	1.145(3)	O(4)−C(4)	1.147(3)
Angles			
P(1)−Fe(1)−C(1)	178.64 (11)	P(1)−Fe(1)−C(2)	90.71(8)
P(1)−Fe(1)−C(3)	90.71(9)	P(1)−Fe(1)−C(4)	89.54(9)
C(1)−Fe(1)−C(2)	89.43(13)	C(1)−Fe(1)−C(3)	90.41(14)
C(1)−Fe(1)−C(4)	89.25(14)	C(2)−Fe(1)−C(3)	118.69(12)
C(2)−Fe(1)−C(4)	123.00(13)	C(3)−Fe(1)−C(4)	118.30(13)
Fe(1)−P(1)−N(1)	116.00(9)	Fe(1)−P(1)−N(2)	116.91(8)
Fe(1)−P(1)−N(3)	117.31(7)	N(1)−P(1)−N(2)	101.38(11)
N(1)−P(1)−N(3)	102.05(12)	N(2)−P(1)−N(3)	100.55(10)
Fe(1)−C(1)−O(1)	179.3(4)	Fe(1)−C(2)−O(2)	178.5(2)
Fe(1)−C(3)−O(3)	177.1(3)	Fe(1)−C(4)−O(4)	177.8(3)

$Fe(CO)_4\{P(NMe_2)_3\}$ (2.245(1) Å)[41] and are comparable to the short Fe−P distances found in $Fe(CO)_4$(ADPO) (2.158(3) Å),[33] $\{(MeNCH_2CH_2NMe)PF\}Fe(CO)_4$ (2.174(1) Å),[42] and $Fe(CO)_4\{(CF_3)_2P{=}N{=}PPh_3\}$ (2.184(1) Å).[43] To our knowledge, the Fe−P distance of 2.1539(5) Å for **7** is the shortest Fe−P distance for an axial-substituted $Fe(CO)_4(PR_3)$ complex, although it is within deviation of that reported for $Fe(CO)_4$(ADPO). Although Fe−P distances are subject to a combination of steric and electronic influences, the short Fe−P bond distances for **7**, **9**, and **10** seem to reflect the π-acceptor properties of the respective phosphine ligands. The order of decreasing π-acidity of **1** > **4** > **3** established from IR data corresponds with the order of increasing Fe−P bond distances in the order **7** < **10** < **9**, as would be expected if increasing π-acidity leads to shortening of the Fe−P bond via an increase in π back-bonding. To assess possible steric influences on the Fe−P distances, crystallographic data were used to determine the cone angles of **1**, **3**, and **4** using the method described by Müller and Mingos.[44] At the crystallographic Fe−P bond distances in **7**, **9**, and **10**, cone angles of 195°, 174°, and 148° were calculated for **1**, **3**, and **4**, respectively. Moloy[13] and Ziolkowski[31] have reported cone angles of 160° and 141°, respectively, for **4**, and we previously reported a cone angle of 191° for **1** based on crystallographic data for Rh(acac)(CO)(**1**).[12] The similar cone angles for **4**, PPh_3 (145°),[45] and $P(NMe_2)_3$ (157°)[45] suggest that the shorter Fe−P distance in **10** compared to those for $Fe(CO)_4(PPh_3)$ and $Fe(CO)_4\{P(NMe_2)_3\}$ is indeed due to the stronger π-acceptor property of **4**. This is qualitatively in agreement with the predicted even shorter Fe−P distance of 2.124 Å for **10**, based on density functional methods of Gonzalez-Blanco and Branchadell.[46] Similarly, the very short Fe−P distance in **7** is attributed to the strong π-acceptor property and the rigid 3-fold symmetry of **1**. Even though **1** has a significantly larger cone angle than even P^tBu_3 (182°),[45] steric repulsion between **1** and the equatorial carbonyls in **7** is minimal since the carbonyls are readily positioned between the planes of the rigid indolyl groups of **1** as observed in Figure 2b.

Axial−Equatorial Carbonyl Exchange in Compounds 7−10. $Fe(CO)_4(PR_3)$ complexes typically undergo rapid intramolecular axial−equatorial carbonyl exchange, even at temperatures as low as −110 °C.[1−9] This exchange is evident by ^{13}C NMR spectroscopy where the carbonyls appear as a single time-averaged doublet due to two-bond $^{13}C-^{31}P$ coupling. Consistent with this precedent, room temperature ^{13}C NMR spectra for **8**, **9**, and **10** each exhibit one doublet resonance at 208.6, 211.4, and 210.9 ppm, respectively. The ^{13}C NMR spectrum of **8** remains unchanged at −80 °C, as does that for **10** as previously reported by Atwood and co-workers.[18] The carbonyl resonance for **9** begins to broaden upon cooling, but decoalescence is not observed and only a single broad resonance remains at −80 °C. Thus, intramolecular rearrangement of axial and equatorial carbonyls in compounds **8**−**10** appears rapid on the NMR time scale.

In contrast to the ^{13}C NMR spectra for compounds **8**−**10**, the room-temperature ^{13}C NMR (100.6 MHz) spectrum of **7** (Figure 5) shows two broad resonances at ∼217 and ∼207 ppm assigned to axial and equatorial carbonyls, respectively. We believe this to be the first observation of resolved axial and equatorial carbonyl resonances in a $Fe(CO)_4L$ complex *at room temperature*. The limiting low-temperature spectrum is reached at −20 °C, with the two resonances sharpened into doublets at 217.3 and 207.1 ppm in a 1:3 ratio (Figure 5). Upon warming

(38) (a) Kilbourn, B. T.; Raeburn, U. A.; Thompson, D. T. *J. Chem. Soc. A* **1969**, 1906. (b) Einstein, F. W. B.; Jones, R. D. G. *J. Chem. Soc., Dalton Trans.* **1972**, 442. (c) Fischer, J.; Mitschler, A.; Ricard, L.; Mathey, F. *J. Chem. Soc., Dalton Trans*. **1980**, 2522. (d) Keiter, R. L.; Rheingold, A. L.; Hamerski, J. J.; Castle, C. K. *Organometallics* **1983**, *2*, 1635. (e) Chernega, A. N.; Antipin, M. Y.; Struchkov, Y. T.; Balitskii, Y. V.; Gololobov, Y. G.; Boldeskul, I. E. *Zh. Obshch. Khim*. **1984**, *54*, 271. (f) Barron, A. R.; Cowley, A. H.; Nunn, C. M. *Acta Crystallogr*. **1988**, *C44*, 750. (g) Wood, G. L.; Duesler, E. N.; Paine, R. T.; Noth, H. *Phosphorus, Sulfur Silicon Relat. Elem*. **1989**, *41*, 267. (h) Kim, T.-J.; Kwon, S.-C.; Kim, Y.-H.; Heo, N. H.; Teeter, M. M.; Yamano, A. *J. Organomet. Chem.* **1991**, *426*, 71. (i) Adams, C. J.; Bruce, M. I.; Horn, E.; Tiekink, E. R. T. *J. Chem. Soc., Dalton Trans*. **1992**, 1157. (j) Dias Rodrigues, A. M. G.; Lechat, J. R.; Francisco, R. H. P. *Acta Crystallogr*. **1992**, *C48*, 159. (k) Dou, D.; Kaufmann, B.; Duesler, E. N.; Chen, T.; Paine, R. T.; Noth, H. *Inorg. Chem*. **1993**, *32*, 3056. (l) Sun, X.; Wong, E. H.; Turnbull, M. M.; Rheingold, A. L.; Waltemire, B. E.; Ostrander, R. L. *Organometallics* **1995**, *14*, 83. (m) Munchenberg, J.; Fischer, A. K.; Thonnessen, H.; Jones, P. G.; Schmutzler, R. *J. Organomet. Chem*. **1997**, *529*, 361. (n) Brunet, J.-J.; Capperucci, A.; Chauvin, R.; Donnadieu, B. *J. Organomet. Chem*. **1997**, *533*, 79. (o) Wit, J. B. M.; van Eijkel, G. T.; de Kanter, F. J. J.; Schakel, M.; Ehlers, A. W.; Lutz, M.; Spek, A. L.; Lammertsma, K. *Angew. Chem., Int. Ed. Engl*. **1999**, *38*, 2596. (p) Dou, D.; Duesler, E. N.; Paine, R. T. *Inorg. Chem*. **1999**, *38*, 788.
(39) Pickardt, J.; Rosch, L.; Schumann, H. *J. Organomet. Chem*. **1976**, *107*, 241.
(40) Riley, P. E.; Davis, R. E. *Inorg. Chem*. **1980**, *19*, 159.
(41) Cowley, A. H.; Davis, R. E.; Remadna, K. *Inorg. Chem*. **1981**, *29*, 2146.
(42) Bennett, D. W.; Neustadt, R. J.; Parry, R. W.; Cagle, F. W. *Acta Crystallogr*. **1978**, *B34*, 3362.
(43) Ang, H. G.; Cai, Y. M.; Koh, L. L.; Kwik, W. L. *J. Chem. Soc., Chem. Commun.* **1991**, 850.
(44) Müller, T. E.; Mingos, D. M. P. *Transition Met. Chem. (N. Y.)* **1995**, *20*, 533.
(45) Tolman, C. A. *Chem. Rev.* **1977**, *77*, 313.
(46) Gonzalez-Blanco, O.; Branchadell, V. *Organometallics* **1997**, *16*, 5556.

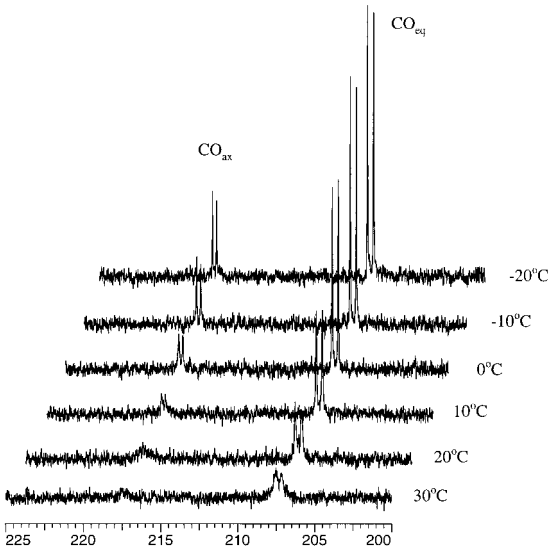

Figure 5. Variable-temperature ^{13}C NMR spectra in the carbonyl region for **7** in CD_2Cl_2 solution.

Table 9. Rate Constants and Activation Parameters for **7**

temp (°C)	rate const (s^{-1})	$\Delta G^{\ddagger}$ (kJ mol^{-1})
−20	12	56.4
−10	18	57.8
0	35	58.6
10	73	59.1
20	135	59.7
30	330	59.6

a toluene-d_8 solution of **7**, we observed that the two broad resonances collapse into the baseline, but even at 90 °C, coalescence of the two resonances was not observed. Coalescence was also not observed in the ^{13}C NMR (50.3 MHz) spectrum obtained at 90 °C even though coalescence should be observed at a lower temperature at lower spectrometer frequency. Room-temperature NMR (^1H, ^{31}P) and IR spectra indicate that no decomposition occurred during the high-temperature NMR experiments; thus decomposition does not account for the unobserved coalescence.

We interpret these NMR observations to indicate an unusually high barrier to intramolecular rearrangement in complex **7**. For comparison, Whitmire and co-workers reported resolution of the axial and equatorial carbonyl resonances in the low-temperature (−85 °C) ^{13}C NMR spectrum of $[Bi\{Fe(CO)_4\}_4]^{3-}$,[10] and similarly, Howell et al. reported observation of the slow-exchange ^{13}C NMR spectrum of $Fe(CO)_4\{P(o\text{-tolyl})_3\}$ at −75 °C.[9] Coalescence was observed for $[Bi\{Fe(CO)_4\}_4]^{3-}$ at −45 °C (90.4 MHz) and for $Fe(CO)_4\{P(o\text{-tolyl})_3\}$ at −40 °C (67.8 MHz), whereas **7** does not coalesce even at 90 °C at the lower spectrometer frequency of 50.3 MHz. Variable-temperature ^{13}C NMR spectra for **7** obtained at 100.6 MHz were simulated using DNMR3 as part of the SPINWORKS software package[47] to yield the exchange rate constants given in Table 9. These simulations suggest $\Delta G^{\ddagger}$ values in the range of 56−60 kJ mol^{-1}, which are considerably higher than the $\Delta G^{\ddagger}$ values of 41.8−39.8 kJ mol^{-1} calculated for the axial−equatorial carbonyl exchange in $Fe(CO)_4\{P(o\text{-tolyl})_3\}$ in the temperature range of −95 to 20 °C. On the basis of a $\Delta G^{\ddagger}$ of approximately 60 kJ mol^{-1} and a computer-simulated exchange rate of 25 000 s^{-1} at coalescence, we estimate a coalescence temperature of approximately 97 °C.[48] This estimated coalescence temperature is consistent with our inability to observe the fast-exchange region for the carbonyl exchange in **7** at 90 °C.

Is it the steric bulk or the electronic properties of **1** that account for this unique behavior of complex **7**? Given the similar donor/acceptor properties of phosphines **1**−**4**, we can dismiss electronic factors as the main contributors to the slowed intramolecular rearrangement for **7** when compounds **8**−**10** remain fluxional even at −80 °C. Steric factors were cited as the reason for slowed axial−equatorial carbonyl exchange in both $[Bi\{Fe(CO)_4\}_4]^{3-}$ and $Fe(CO)_4\{P(o\text{-tolyl})_3\}$[9,10] as well as for differences in rearrangement rates in a series of related $Co(CO)_4(EX_3)$ complexes.[49] There appears to be some correlation between the phosphine cone angle and the tendency for rearrangement in the corresponding $Fe(CO)_4(PR_3)$ complex. Phosphines with cone angles[45] less than approximately 175° appear to have fluxional $Fe(CO)_4(PR_3)$ complexes at −80 °C. This holds true for $P(OMe)_3$ (107°), PMe_3 (118°), $P(OPh)_3$ (128°), PPh_3 (145°), **4** (141−160°), $P(4\text{-}CF_3C_6H_4)_3$ (164°), $P(3\text{-}CF_3C_6H_4)_3$ (164°), PCy_3(170°), and **3** (174°),[5,6,36] although complex **9** shows some broadening of the carbonyl ^{13}C resonance at −80 °C. In $Fe(CO)_4\{P(o\text{-tolyl})_3\}$ and **7**, the only examples where slowed intermolecular rearrangement is observed, $P(o\text{-tolyl})_3$ and **1** have cone angles of 194° and 195°, respectively. The cone angle is not a complete descriptor of steric influence, as can be seen by the very different rearrangements rates for $Fe(CO)_4\{P(o\text{-tolyl})_3\}$ and **7** despite the nearly identical cone angles for $P(o\text{-tolyl})_3$ and **1**. We attribute the more hindered rearrangement in **7** to the rigid 3-fold nature of **1**. The three equatorial carbonyls are readily situated between the planes of the indolyl rings when **1** occupies an axial position in **7**, but **1** will exert significant steric repulsion on carbonyls in the square pyramidal intermediates of plausible Berry pseudorotation (phosphine basal) and umbrella processes (phosphine apical), as well as become a steric hindrance to turnstile rotation.[49] Rotation about the P−C bond axes in $P(o\text{-tolyl})_3$ may allow a lower energy pathway for axial−equatorial carbonyl exchange in $Fe(CO)_4\{P(o\text{-tolyl})_3\}$. In fact, Howell et al. have cited NMR data which suggest that carbonyl exchange is dependent on the conformation of the $P(o\text{-tolyl})_3$ ligand and, possibly, that carbonyl exchange is concerted with P−C bond rotation.[9] These processes are not available in **7** due to the rigid bicyclic framework of **1**.

Conclusions

Complex **7** is only the second example in which slowed axial−equatorial carbonyl exchange in a $Fe(CO)_4(PR_3)$ complex has been observed by ^{13}C NMR spectroscopy and is the first complex in which this process is observed to be slow at room temperature. In an effort to elucidate steric and electronic factors responsible for the hindered carbonyl exchange in **7**, we synthesized the constrained π-acid **2**. Ligand **2** is a weak σ-base and a potent π-acid and is electronically comparable to **1** but has considerably less steric bulk. Constraint of the N−P−N angles in **2** by the tri(pyrrolyl)methane framework accounts for the decreased σ-basicity and increased π-acidity when compared

(47) Marat, K. *SPINWORKS 1.2: Program for NMR Simulation*; University of Manitoba: Winnepeg, Manitoba, Canada.

(48) (a) Wilkins, R. G. *Kinetics and Mechanism of Reactions of Transition Metal Complexes*, 2nd ed.; VCH Publishers: Weinheim, Germany, 1991; Chapter 2. (b) Günther, H. *NMR Spectroscopy: An Introduction*; John Wiley & Sons: New York, 1980; Chapter 8.

(49) Lichtenberger, D. L.; Brown, T. L. *J. Am. Chem. Soc.* **1977**, *99*, 8187 and references therein.

with **4**. Analogous to ligand **1**, the P−N bonds of **2** are stable to hydrolysis and alcoholysis.

Ligands **2**−**4** were used to synthesize **8**, **9**, and **10**. Unlike complex **7**, complexes **8**−**10** remain fluxional at −80 °C. The similar electronic properties of compounds **1**−**4** argue against ligand electronic properties strongly influencing the hindered exchange in complex **7**. Thus, we attribute the hindered rearrangment in **7** to the steric bulk and rigid 3-fold symmetry of **1**. Further examination of the coordination chemistry and catalytic applications of compounds **1**−**3** and related ligands is ongoing.

Acknowledgment. Financial support for T.S.B. was generously provided by The University of Toledo in the form of start-up funds to M.R.M. We thank Kristin Kirschbaum for instruction on the operation of the Siemens CCD diffractometer. Drs. Yong Wah Kim and Kirk Marat are acknowledged for useful suggestions on the simulation of the variable-temperature NMR spectra for **7**.

Supporting Information Available: X-ray crystallographic files in CIF format for the structure determinations of **2**, **7**, **9**, and **10**. This material is available free of charge via the Internet at http://pubs.acs.org.

IC001372B